Sciencexpress Reports

# The Crust of the Moon as Seen by GRAIL

**Mark A. Wieczorek,[1]* Gregory A. Neumann,[2] Francis Nimmo,[3] Walter S. Kiefer,[4] G. Jeffrey Taylor,[5] H. Jay Melosh,[6] Roger J. Phillips,[7] Sean C. Solomon,[8,9] Jeffrey C. Andrews-Hanna,[10] Sami W. Asmar,[11] Alexander S. Konopliv,[11] Frank G. Lemoine,[2] David E. Smith,[12] Michael M. Watkins,[11] James G. Williams,[11] Maria T. Zuber[12]**

[1]Institut de Physique du Globe de Paris, Sorbonne Paris Cité, Univ Paris Diderot, Case 7011, Bâtiment Lamarck A, 5, rue Thomas Mann, 75205 Paris Cedex 13, France. [2]Solar System Exploration Division, NASA Goddard Space Flight Center, Greenbelt, MD 20771, USA. [3]Department of Earth and Planetary Sciences, University of California, Santa Cruz, 1156 High Street, Santa Cruz, CA 95064, USA. [4]Lunar and Planetary Institute, Houston, TX 77058, USA. [5]Hawaii Institute of Geophysics and Planetology, University of Hawaii, Honolulu, HI 96822, USA. [6]Department of Earth and Atmospheric Sciences, Purdue University, 550 Stadium Mall Drive, West Lafayette, IN 47907, USA. [7]Planetary Science Directorate, Southwest Research Institute, Boulder, CO 80302, USA. [8]Department of Terrestrial Magnetism, Carnegie Institution of Washington, Washington, DC 20015, USA. [9]Lamont-Doherty Earth Observatory, Columbia University, Palisades, NY 10964, USA. [10]Department of Geophysics, Colorado School of Mines, 1500 Illinois Sreet, Golden, CO 80401–1887, USA. [11]Jet Propulsion Laboratory, California Institute of Technology, Pasadena, CA 91109, USA. [12]Department of Earth, Atmospheric and Planetary Sciences, Massachusetts Institute of Technology, Cambridge, MA 02139–4307, USA.

*To whom correspondence should be addressed. E-mail: wieczor@ipgp.fr

**High-resolution gravity data obtained from the dual Gravity Recovery and Interior Laboratory (GRAIL) spacecraft show that the bulk density of the Moon's highlands crust is 2550 kg m$^{-3}$, substantially lower than generally assumed. When combined with remote sensing and sample data, this density implies an average crustal porosity of 12% to depths of at least a few kilometers. Lateral variations in crustal porosity correlate with the largest impact basins, whereas lateral variations in crustal density correlate with crustal composition. The low bulk crustal density allows construction of a global crustal thickness model that satisfies the Apollo seismic constraints, and with an average crustal thickness between 34 and 43 km, the bulk refractory element composition of the Moon is not required to be enriched with respect to that of Earth.**

The nature of the lunar crust provides crucial information on the Moon's origin and subsequent evolution. Because the crust is composed largely of anorthositic materials (*1*), its average thickness is key to determining the bulk silicate composition of the Moon (*2*, *3*), and consequently, whether the Moon was derived largely from Earth materials or from the giant impactor that is believed to have formed the Earth-Moon system (*4*, *5*). Following formation, the crust of the Moon suffered the consequences of 4.5 billion years of impact cratering. The Moon is the nearest and most accessible planetary body to study the largest of these catastrophic events, which were common during early solar system evolution (*6*, *7*). In addition, it is an ideal laboratory for investigating the cumulative effects of the more frequent smaller impact events. Spatial variations in the Moon's gravity field are reflective of subsurface density variations, and the high-resolution measurements provided by NASA's Gravity Recovery and Interior Laboratory (GRAIL) mission (*8*) are particularly useful for investigating these issues.

Previous gravity investigations of the Moon have made use of data derived from radio tracking of orbiting spacecraft, but these studies were frustrated by the low and uneven spatial resolution of the available gravity models (*9*, *10*). GRAIL consists of two co-orbiting spacecraft that are obtaining continuous high-resolution gravity measurements by intersatellite ranging over both the near- and far-side hemispheres of Earth's natural satellite (*8*). Gravity models at the end of the primary mission resolve wavelengths as fine as 26 km, which is more than a factor of 4 times less than any previous global model. The mass anomalies associated with the Moon's surface topography are one of the most prominent signals seen by GRAIL (*11*), and because the measured gravity signal at short wavelengths is not affected by the compensating effects of lithospheric flexure, these data offer an opportunity to determine unambiguously the bulk density of the lunar crust. The density of the crust is a fundamental property required for geophysical studies of the Moon, and it also provides important information on crustal composition over depth scales that are greater than those of most other remote sensing techniques.

The deflection of the crust-mantle interface in response to surface loads makes only a negligible contribution to the observed gravity field beyond spherical harmonic degree and order 150 (*12*). At these wavelengths, if the gravitational contribution of the surface relief were removed with the correct reduction density, the remaining signal (the Bouguer anomaly) would be zero if there were no other density anomalies present in the crust. An estimate of the crustal density can be obtained by minimizing the correlation between surface topography and Bouguer gravity. To exclude complicating flexural signals, and to interpret only that portion of the gravity field that is well resolved, we first filtered the gravity and topography to include spherical harmonic degrees between 150 and 310. Gravity and topography over the lunar maria, areas of generally low elevation resurfaced by high density basaltic lava flows, were excluded from analysis, because their presence would bias the bulk density determination.

For our analyses, the correlation coefficient of the Bouguer gravity and surface topography was minimized using data within circles that span 12° of latitude. Analyses were excluded when more than 5% of the region was covered by mare basalt, and when the minimum correlation coefficient fell outside the 95% confidence limits as estimated from Monte Carlo simulations that utilized the gravity coefficient uncertainties. The average density of the highlands crust was found to be 2550 kg m$^{-3}$, and individual density uncertainties were on average 18 kg m$^{-3}$. As shown in Fig. 1, substantial lateral variations in crustal density exist with amplitudes of ±250 kg m$^{-3}$. The largest positive excursions are associated with the 2000-km diameter South Pole-Aitken basin on the Moon's farside hemisphere, a region that has been shown by remote sensing data to be composed of rocks that are considerably more mafic, and thus denser, than the surrounding anorthositic highlands (*13*). Extensive regions with densities lower than average are found surrounding the impact basins Orientale and Moscoviense, which are the two largest young impact basins on the Moon's farside hemisphere. The bulk density determinations are robust to changes in size of the analysis region by a factor of two, and are robust to changes in the spectral filter limits by more than ±50 in harmonic degree. Nearly identical bulk densities are

obtained with both a global and localized spectral admittance approach (figs. S6 and S7).

The bulk crustal densities obtained from GRAIL are considerably lower than the values of 2800 to 2900 kg $m^{-3}$ that are typically adopted for geophysical models of anorthositic crustal materials (*14*). We attribute the low densities to impact-induced fractures and brecciation. From an empirical relation between the grain density of lunar rocks and their concentration of FeO and $TiO_2$ (*15*), along with surface elemental abundances derived from gamma-ray spectroscopy (*16*), grain densities of lunar surface materials may be estimated globally with a precision and spatial resolution that are comparable to those of the GRAIL bulk density measurements (fig. S3). If the surface composition of the Moon is representative of the underlying crust, the implied porosity is on average 12% and varies regionally from about 4 to 21% (Fig. 2). These values are consistent with, though somewhat larger than, estimates made from earlier longer-wavelength gravity field observations and a lithospheric flexure model (*15*). The crustal porosities in the interiors of many impact basins are lower than their surroundings, consistent with a reduction in pore space by high post-impact temperatures, which can exceed the solidus temperature. In contrast, the porosities immediately exterior to many basins are higher than their surroundings, a result consistent with the generation of increased porosity by the ballistic deposition of impact ejecta and the passage of impact-generated shock waves.

If the crustal density were constant at all depths greater than the lowest level of surface elevation, our bulk density estimates would represent an average over the depths sampled by the topographic relief, on average about 4 km. Because the deeper crust would not generate lateral gravity variations under such a scenario, this depth should be considered a minimum estimate for the depth scale of the GRAIL density determinations. If crustal porosity were solely a function of depth below the surface, the depth scale could be constrained using the relationship between gravity and topography in the spectral domain, since deep and short-wavelength mass anomalies are attenuated with altitude faster than shallower and longer-wavelength anomalies. We investigated two models: one in which the porosity decreases exponentially with depth below the surface, and another in which a porous layer of constant thickness and constant porosity overlies a non-porous basement (*12*). The upper bound on both depth scales, at one standard deviation or 1-σ, is largely unconstrained, with values greater than 30 km able to fit the observations in most regions. Lower bounds at 1-σ for the two depth scales were constrained to lie between about 0 and 31 km. These results imply that at least some regions of the highlands have substantial porosity extending to depths of tens of kilometers, and perhaps into the uppermost mantle.

Our density and porosity estimates are broadly consistent with laboratory measurements of lunar feldspathic meteorites and feldspathic rocks collected during the Apollo missions. The average bulk density of the most reliable of these measurements is 2580 ± 170 kg $m^{-3}$ (*12, 17*), and the porosities of these samples vary from about 2 to 22% and have an average of 8.6 ± 5.3%. Ordinary chondrite meteorites have a similar range of porosities as the lunar samples, a result of impact-induced microfractures (*18*). A 1.5-km drill core in the Chicxulub impact basin on Earth shows that impact deposits have porosities between 5 and 24%, whereas the basement rocks contain porosities up to 21% (*19*). Gravity data over the Ries, Tvären, and Granby terrestrial impact craters (with diameters of 23, 3, and 2 km) imply values of 10-15% excess porosity 1 km below the surface (*20*, *21*), and for the Ries, about 7% porosity at 2 km depth. Whereas the impact-induced porosities associated with the terrestrial craters are a result of individual events, on the Moon, each region of the crust has been affected by numerous impacts.

Pore closure at depth within the Moon is likely to occur by viscous deformation at elevated temperatures; this decrease occurs over a narrow depth interval (<5 km) (fig. S12) because of the strong temperature-dependence of viscosity (*22*). From representative temperature gradients over 4 billion years, and taking into account the reduced thermal conductivity of porous rock, this transition depth is predicted to lie between 40 and 85 km below the surface, depending on the rheology and heat fluxes assumed. Where the crust is thinner than these values, porosity could exist in the underlying mantle. S-wave velocity profiles derived from the Apollo seismic data (*23*) suggest that porosity extends to depths up to 15 km below the crust-mantle interface, consistent with this interpretation.

With our constraints on crustal density and porosity, we constructed a global crustal thickness model from GRAIL gravity and Lunar Reconnaissance Orbiter (LRO) topography (*24*) data. Our model accounts for the gravitational signatures of the surface relief, relief along the crust-mantle interface, and the signal that arises from lateral variations in crustal grain density as predicted by remote sensing data (*12*). Crustal densities beneath the mare basalts were extrapolated from the surrounding highland values, and because we neglect the comparatively thin surficial layer of dense basalt (*14*), the total crustal thicknesses will be biased locally, but by no more than a few kilometers. As constraints to our model, we used seismically determined thicknesses of either 30 (*23*) or 38 (*25*) km near the Apollo 12 and 14 landing sites, and we assumed a minimum crustal thickness of less than 1 km because at least one of the giant impact basins should have excavated through the entire crust (*14*, *26*). Given a porosity model of the crust, we obtained a single model that fits the observations by varying the average crustal thickness and mantle density. Because some of the short-wavelength gravity signal is the result of unmodeled crustal signals, our inversions make use of a spectral low-pass filter (*27*) near degree 80, yielding a spatial resolution that is 60% better than previous models (*28*). Remote sensing data of impact crater central peaks imply some subsurface compositional variability but do not require broad compositional layering (*29*), at least consistent with our use of a model that is uniform in composition with depth.

For a first set of models, we assumed that porosity was a function of depth below the surface. With a mantle grain density of 3360 kg $m^{-3}$ (*30*), it is not possible to fit simultaneously the seismic and minimum thickness constraints as a result of the relatively small density contrast at the crust-mantle interface (*12*). For a second set of models, we assumed that the porosity of the entire crust was constant with depth. With 12% porosity and a 30-km crustal thickness near the Apollo 12 and 14 landing sites, a solution is found with an average crustal thickness of 34 km and a mantle density of 3220 kg $m^{-3}$ (Fig. 3). For a 38-km crustal-thickness constraint, values of 43 km and 3150 kg $m^{-3}$ are found, respectively. By reducing the porosity to 7%, the mantle density increases by about 150 kg $m^{-3}$, but the average crustal thickness remains unchanged. Identical average crustal thicknesses are obtained for a crustal density map extrapolated from Fig. 1. The mantle densities should be considered representative to the greatest depths of the base of the crust (~ 80 km below the surface), and if the grain density of mantle materials is 3360 kg $m^{-3}$, the uppermost mantle could have a porosity between 0 and 6%, consistent with our porosity evolution model (*12*).

Before GRAIL, the average thickness of the Moon's crust was thought to be close to 50 km (*14*, *28*) (*12*). Published estimates for the bulk silicate abundance of the refractory element aluminum, as summarized in table 1 of Taylor *et. al* (*3*), fall into two categories: One group indicates that the Moon contains the same abundance as Earth, whereas the other suggests at least a 50% enrichment. We used our average crustal thickness with assumptions on crustal composition that maximize of the total $Al_2O_3$ in the crust to test the limits of the refractory enrichment hypothesis. If the lunar crust consists of an upper megaregolith layer 5-km thick containing 28 wt.% $Al_2O_3$ (*3*), a value based largely on lunar highland meteorite compositions, with the remainder being nearly pure anorthosite, 34 wt.% $Al_2O_3$ (*1*), we calculate that a 34-km-thick crust contributes 1.7 wt.% to the total bulk silicate abundance of $Al_2O_3$ for a crustal porosity of 7%. A 43-km-thick crust contributes 2.1 wt.%. The inclusion of more mafic materials in the lower crust would act to reduce

the total abundance of aluminum in the crust. In order for bulk lunar silicate aluminum abundances to match those for Earth (4 wt.% $Al_2O_3$), the lunar mantle would need to contain 1.9-2.4 wt.% $Al_2O_3$, whereas a 50% enrichment in refractory elements would require 4.1-4.5 wt.% $Al_2O_3$. Petrologic assessments indicate mantle $Al_2O_3$ abundances close to 1-2 wt.% (*31*), supporting a lunar refractory element composition similar to that of Earth. Estimates of $Al_2O_3$ derived from modeling the Apollo seismic data have a broad range, from 2.3-3.1 wt.% for the entire mantle (*32*), to 2.0 to 6.7 wt.% for the upper and lower mantle (*33*), respectively. Although further constraints on the composition of the deep lunar mantle are needed, the modest contribution to the bulk lunar $Al_2O_3$ from the crust does not require the Moon to be enriched in refractory elements.

Crustal thickness variations on the Moon are dominated by impact basins with diameters from 200 to 2000 km. With a thinner crust, it becomes increasingly probable that several of the largest impact events excavated through the entire crustal column and into the mantle (*14*). Two impact basins have interior thicknesses near zero (Moscoviense and Crisium), and three others have thicknesses that are less than 5 km (Humboldtianum, Apollo, and Poincaré). Remote sensing data show atypical exposures of olivine-rich materials surrounding some lunar impact basins that could represent an admixture of crustal materials with excavated mantle materials (*26*), and the most prominent of these are associated with the Crisium, Moscoviense, and Humboldtianum basins. Our crustal thickness model strengthens the hypothesis that these impact events excavated into the mantle.

Because the crust of the Moon has experienced only limited volcanic modification, and in addition has not experienced aqueous or aeolian erosion, the Moon is an ideal recorder of processes that must have affected the crusts of all terrestrial planets early in their evolution. Large impact events were common in the first billion years of solar system history, and the crusts of the terrestrial planets would have been fractured to great depths, as was the Moon. For Earth and Mars, this porosity could have hosted substantial quantities of ground water over geologic time (*34*). For planets generally lacking groundwater, such as Mercury, crustal porosity may have sharply reduced the effective thermal conductivity, hindering the escape of heat to the surface and affecting the planet's thermal and magmatic evolution (*35*).

**References and Notes**


1. S. Yamamoto *et al*., Massive layer of pure anorthosite on the Moon. *Geophys. Res. Lett.* **39**, L13201 (2012). doi:10.1029/2012GL052098
2. P. H. Warren, "New" lunar meteorites: Implications for composition of the global lunar surface, lunar crust, and the bulk Moon. *Meteorit. Planet. Sci.* **40**, 477 (2005). doi:10.1111/j.1945-5100.2005.tb00395.x
3. S. R. Taylor, G. J. Taylor, L. A. Taylor, The Moon: A Taylor perspective. *Geochim. Cosmochim. Acta* **70**, 5904 (2006). doi:10.1016/j.gca.2006.06.262
4. R. M. Canup, Forming a Moon with an Earth-like composition via a giant impact. *Science* **338**, 1052 (2012). doi:10.1126/science.1226073 Medline
5. M. Cuk, S. T. Stewart, Making the moon from a fast-spinning Earth: A giant impact followed by resonant despinning. *Science* **338**, 1047 (2012). Medline
6. W. F. Bottke *et al*., An Archaean heavy bombardment from a destabilized extension of the asteroid belt. *Nature* **485**, 78 (2012). doi:10.1038/nature10967 Medline
7. C. I. Fassett *et al*., Lunar impact basins: Stratigraphy, sequence and ages from superposed impact crater populations measured from Lunar Orbiter Laser Altimeter (LOLA) data. *J. Geophys. Res.* **117**, E00H06 (2012). doi:10.1029/2011JE003951
8. M. T. Zuber *et al*., Gravity Recovery and Interior Laboratory (GRAIL): Mapping the lunar interior from crust to core. *Space Sci. Rev.* (2012); doi:10.1007/s11214-012-9952-7
9. A. S. Konopliv, S. W. Asmar, D. N. Yuan, Recent gravity models as a result of the Lunar Prospector mission. *Icarus* **150**, 1 (2001). doi:10.1006/icar.2000.6573
10. K. Matsumoto *et al*., An improved lunar gravity field model from SELENE and historical tracking data: Revealing the farside gravity features. *J. Geophys. Res.* **115**, (E6), E06007 (2010). doi:10.1029/2009JE003499
11. M. T. Zuber *et al*., Gravity field of the Moon from the Gravity Recovery and Interior Laboratory (GRAIL) mission. *Science* (2012); published online 5 December 2012; 10.1126/science.1231507
12. Methods and additional materials are available as supplementary materials on *Science* Online.
13. P. Lucey *et al*., *New Views of the Moon*, B. J. Jolliff, M. A. Wieczorek, C. K. Shearer, C. R. Neal, Eds., *Rev. Mineral. Geochem.* (Mineral. Soc. Am., 2006), vol. 60, pp. 83–219.
14. M. A. Wieczorek *et al*., in *New Views of the Moon*, B. J. Jolliff, M. A. Wieczorek, C. K. Shearer, C. R. Neal, Eds., *Rev. Mineral. Geochem.* (Mineral. Soc. Am., 2006), vol. 60, pp. 221–364.
15. Q. Huang, M. A. Wieczorek, Density and porosity of the lunar crust from gravity and topography. *J. Geophys. Res.* **117**, (E5), E05003 (2012). doi:10.1029/2012JE004062
16. T. H. Prettyman *et al*., Elemental composition of the lunar surface: Analysis of gamma ray spectroscopy data from Lunar Prospector. *J. Geophys. Res.* **111**, (E12), E12007 (2006). doi:10.1029/2005JE002656
17. W. Kiefer, R. J. Macke, D. T. Britt, A. J. Irving, G. J. Consolmagno, The density and porosity of lunar rocks. *Geophys. Res. Lett.* **39**, L07201 (2012). doi:10.1029/2012GL051319
18. G. Consolmagno, D. Britt, R. Macke, The significance of meteorite density and porosity. *Chemie der Erde-Geochemistry* **68**, 1 (2008). doi:10.1016/j.chemer.2008.01.003
19. T. Elbra, L. J. Pesonen, Physical properties of the Yaxcopoil-1 deep drill core, Chicxulub impact structure, Mexico. *Meteorit. Planet. Sci.* **46**, 1640 (2011). doi:10.1111/j.1945-5100.2011.01253.x
20. J. Pohl, D. Stoeffler, H. Gall, K. Ernstson, in *Impact and Explosion Cratering: Planetary and Terrestrial Implications*, D. J. Roddy, R. O. Pepin, R. B. Merrill, Eds. (Pergamon Press, New York, 1977), pp. 343–404.
21. H. Henkel, T. C. Ekneligoda, S. Aaro, The extent of impact induced fracturing from gravity modeling of the Granby and Tvären simple craters. *Tectonophysics* **485**, 290 (2010). doi:10.1016/j.tecto.2010.01.008
22. F. Nimmo, R. T. Pappalardo, B. Giese, On the origins of band topography, Europa. *Icarus* **166**, 21 (2003). doi:10.1016/j.icarus.2003.08.002
23. P. Lognonné, J. Gagnepain-Beyneix, H. Chenet, A new seismic model of the Moon: Implications for structure, thermal evolution and formation of the Moon. *Earth Planet. Sci. Lett.* **211**, 27 (2003). doi:10.1016/S0012-821X(03)00172-9
24. D. E. Smith *et al*., Initial observations from the Lunar Orbiter Laser Altimeter (LOLA). *Geophys. Res. Lett.* **37**, L18204 (2010). doi:10.1029/2010GL043751
25. A. Khan, K. Mosegaard, An inquiry into the lunar interior: A nonlinear inversion of the Apollo lunar seismic data. *J. Geophys. Res.* **107**, (E6), 5036 (2002). doi:10.1029/2001JE001658
26. S. Yamamoto *et al*., Possible mantle origin of olivine around lunar impact basins detected by SELENE. *Nat. Geosci.* **3**, 533 (2010). doi:10.1038/ngeo897
27. M. A. Wieczorek, R. J. Phillips, Potential anomalies on a sphere: Applications to the thickness of the lunar crust. *J. Geophys. Res.* **103**, (E1), 1715 (1998). doi:10.1029/97JE03136
28. Y. Ishihara *et al*., Crustal thickness of the Moon: Implications for farside basin structures. *Geophys. Res. Lett.* **36**, L19202 (2009). doi:10.1029/2009GL039708
29. J. T. S. Cahill, P. G. Lucey, M. A. Wieczorek, Compositional variations of the lunar crust: Results from radiative transfer modeling of central peak spectra. *J. Geophys. Res.* **114**, (E9), E09001 (2009). doi:10.1029/2008JE003282
30. R. Garcia, J. Gagnepain-Beyneix, S. Chevrot, P. Lognonné, Very preliminary reference Moon model. *Phys. Earth Planet. Inter.* **188**, 96 (2011). doi:10.1016/j.pepi.2011.06.015
31. S. Mueller, G. J. Taylor, R. J. Phillips, Lunar composition: A geophysical and petrological synthesis. *J. Geophys. Res.* **93**, (B6), 6338 (1988). doi:10.1029/JB093iB06p06338
32. A. Khan, J. A. D. Connolly, J. Maclennan, K. Mosegaard, Joint inversion of seismic and gravity data for lunar composition and thermal state. *Geophys. J. Int.* **168**, 243 (2007). doi:10.1111/j.1365-246X.2006.03200.x
33. O. L. Kuskov, V. A. Kronrod, Constitution of the Moon. *Phys. Earth Planet. Inter.* **107**, 285 (1998). doi:10.1016/S0031-9201(98)00082-X
34. S. M. Clifford, A model for the hydrologic and climatic behavior of water on

Mars. *J. Geophys. Res.* **98**, (E6), 10973 (1993). doi:10.1029/93JE00225
35. S. Schumacher, D. Breuer, Influence of a variable thermal conductivity on the thermochemical evolution of Mars. *J. Geophys. Res.* **111**, (E2), E02006 (2006). doi:10.1029/2005JE002429
36. M. A. Wieczorek, Gravity and topography of the terrestrial planets, in *Treatise on Geophyics*, vol. 10, T. Spohn, and G. Schubert, Eds. (Elsevier-Pergamon, Oxford, 2007), pp. 165–206, doi:10.1016/j.icarus.2007.10.026.
37. D. L. Turcotte, R. J. Willemann, W. F. Haxby, J. Norberry, Role of membrane stresses in the support of planetary topography. *J. Geophys. Res.* **86**, (B5), 3951 (1981). doi:10.1029/JB086iB05p03951
38. D. E. Wilhelms, *The Geologic History of the Moon*, U.S. Geol. Surv. Spec. Pap. 1348, (U.S. Geological Survey, Washington, DC, 1987).
39. H. J. Melosh, *Impact Cratering: A Geologic Process* (Oxford Univ. Press, New York, 1989).
40. M. A. Wieczorek, F. J. Simons, Localized spectral analysis on the sphere. *Geophys. J. Int.* **162**, 655 (2005). doi:10.1111/j.1365-246X.2005.02687.x
41. F. J. Simons, F. A. Dahlen, M. A. Wieczorek, Spatiospectral concentration on a sphere. *SIAM Rev.* **48**, 504 (2006). doi:10.1137/S0036144504445765
42. M. A. Wieczorek, F. J. Simons, Minimum-variance multitaper spectral estimation on the sphere. *J. Fourier Anal. Appl.* **13**, 665 (2007). doi:10.1007/s00041-006-6904-1
43. W. S. Kiefer, R. J. Macke, D. T. Britt, A. J. Irving, G. J. Consolmagno, Density and porosity of lunar feldspathic rocks and implications for lunar gravity modeling, *Second Conf. Lunar Highlands Crust*, abstract 9006 (Lunar and Planetary Institute, Houston, TX, 2012).
44. R. L. Korotev, Lunar geochemistry as told by lunar meteorites. *Chemie der Erde Geochemistry* **65**, 297 (2005). doi:10.1016/j.chemer.2005.07.001
45. M. Ohtake *et al*., Asymmetric crustal growth on the Moon indicated by primitive farside highland materials. *Nat. Geosci*. **5**, 384 (2012). doi:10.1038/ngeo1458
46. G. L. Nord, Jr., J. M. Christie, J. S. Lally, A. H. Heuer, The thermal and deformational history of Apollo 15418: A partly shock-melted lunar breccia. *Moon* **17**, 217 (1977). doi:10.1007/BF00562197
47. G. Ryder, Lunar anorthosite 60025, the petrogenesis of lunar anorthosites, and the composition of the Moon. *Geochim. Cosmochim. Acta* **46**, 1591 (1982). doi:10.1016/0016-7037(82)90316-7
48. D. Stoeffler, S. Schulien, R. Ostertag, Rock 61016: Multiphase shock and crystallization history of a polymict troctolitic-anorthositic breccia. *Proc. Lunar Planet. Sci. Conf.* **6**, 673 (1975).
49. J. T. Cahill *et al*., Petrogenesis of lunar highlands meteorites: Dhofar 025, Dhofar 081 Dar al Gani 262, and Dar al Gani 400. *Meteorit. Planet. Sci.* **39**, 503 (2004). doi:10.1111/j.1945-5100.2004.tb00916.x
50. I. J. Daubar, D. A. Kring, T. D. Swindle, A. J. T. Jull, Northwest Africa 482: A crystalline impact-melt breccia from the lunar highlands. *Meteorit. Planet. Sci.* **37**, 1797 (2002). doi:10.1111/j.1945-5100.2002.tb01164.x
51. J. A. Hudgins, S. P. Kelley, R. L. Korotev, J. G. Spray, Mineralogy, geochemistry, and 40Ar-39Ar geochronology of lunar granulitic breccia Northwest Africa 3163 and paired stones: Comparisons with Apollo samples. *Geochim. Cosmochim. Acta* **75**, 2865 (2011). doi:10.1016/j.gca.2011.02.035
52. R. L. Korotev, B. L. Jolliff, R. A. Zeigler, J. J. Gillis, L. A. Haskin, Feldspathic lunar meteorites and their implications for compositional remote sensing of the lunar surface and the composition of the lunar crust. *Geochim. Cosmochim. Acta* **67**, 4895 (2003). doi:10.1016/j.gca.2003.08.001
53. R. L. Korotev, R. A. Zeigler, B. L. Jolliff, Feldspathic lunar meteorites Pecora Escarpment 02007 and Dhofar 489: Contamination of the surface of the lunar highlands by postbasin impacts. *Geochim. Cosmochim. Acta* **70**, 5935 (2006). doi:10.1016/j.gca.2006.09.016
54. R. L. Korotev, R. A. Zeigler, B. L. Jolliff, A. J. Irvin, T. E. Bunch, Compositional and lithological diversity among brecciated lunar meteorites of intermediate iron concentration. *Meteorit. Planet. Sci.* **44**, 1287 (2009). doi:10.1111/j.1945-5100.2009.tb01223.x
55. R. L. Korotev, Lunar meteorites from Oman. *Meteorit. Planet. Sci.* **47**, 1365 (2012). doi:10.1111/j.1945-5100.2012.01393.x
56. A. K. Sokol *et al*., Geochemistry, petrology and ages of the lunar meteorites Kalahari 008 and 009: New constraints on early lunar evolution. *Geochim. Cosmochim. Acta* **72**, 4845 (2008). doi:10.1016/j.gca.2008.07.012
57. P. H. Warren, F. Ulff-Møller, G. W. Kallemeyn, "New" lunar meteorites: Impact melt and regolith breccias and large-scale heterogeneities of the upper lunar crust. *Meteorit. Planet. Sci.* **40**, 989 (2005). doi:10.1111/j.1945-5100.2005.tb00169.x
58. R. J. Macke, D. T. Britt, G. J. Consolmagno, Analysis of systematic error in "bead method" measurements of meteorite bulk volume and density. *Planet. Space Sci.* **58**, 421 (2010). doi:10.1016/j.pss.2009.11.006
59. P. H. Warren, K. L. Rasmussen, Megaregolith insulation, internal temperatures, and bulk uranium content of the Moon. *J. Geophys. Res.* **92**, (B5), 3453 (1987). doi:10.1029/JB092iB05p03453
60. M. Talwani, G. Thompson, B. Dent, H.-G. Kahle, S. Buck, Traverse gravimeter experiment, in *Apollo 17: Preliminary Science Report* (1973), *NASA Special Publication* 330, pp. 13.1–13.7.
61. A. C. Fowler, A mathematical model of magma transport in the asthenosphere. *Geophys. Astrophys. Fluid Dyn.* **33**, 63 (1985). doi:10.1080/03091928508245423
62. J. Eluszkiewicz, Dim prospects for radar detection of Europa's ocean. *Icarus* **170**, 234 (2004). doi:10.1016/j.icarus.2004.02.011
63. E. Rybacki, G. Dresen, Amorphous ice and the behavior of cometary nuclei. *J. Geophys. Res.* **105**, 26017 (2000). doi:10.1029/2000JB900223
64. S. Karato, P. Wu, Rheology of the upper mantle: A synthesis. *Science* **260**, 771 (1993). doi:10.1126/science.260.5109.771 Medline
65. R. Smoluchowski, Amorphous ice and the behavior of cometary nuclei. *Astrophys. J.* **244**, L31 (1981). doi:10.1086/183473
66. J. R. Driscoll, D. M. Healy, Computing Fourier transforms and convolutions on the 2-sphere. *Adv. Appl. Math.* **15**, 202 (1994). doi:10.1006/aama.1994.1008
67. M. N. Toksöz, A. M. Dainty, S. C. Solomon, K. R. Anderson, Structure of the Moon. *Rev. Geophys.* **12**, 539 (1974). doi:10.1029/RG012i004p00539
68. M. T. Zuber, D. E. Smith, F. G. Lemoine, G. A. Neumann, The shape and internal structure of the moon from the Clementine mission. *Science* **266**, 1839 (1994). doi:10.1126/science.266.5192.1839 Medline
69. G. A. Neumann, M. T. Zuber, D. E. Smith, F. G. Lemoine, The lunar crust: Global structure and signature of major basins. *J. Geophys. Res.* **101**, (E7), 16,841 (1996). doi:10.1029/96JE01246
70. A. Khan, K. Mosegaard, K. K. L. Rasmussen, A new seismic velocity model for the Moon from a Monte Carlo inversion of the Apollo lunar seismic data. *Geophys. Res. Lett.* **27**, 1591 (2000). doi:10.1029/1999GL008452
71. J. Gagnepain-Beyneix, P. Lognonné, H. Chenet, D. Lombardi, T. Spohn, A seismic model of the lunar mantle and constraints on temperature and mineralogy. *Phys. Earth Planet. Inter.* **159**, 140 (2006). doi:10.1016/j.pepi.2006.05.009
72. H. Chenet, P. Lognonn'e, M. Wieczorek, H. Mizutani, Lateral variations of lunar crustal thickness from the Apollo seismic data set. *Earth Planet. Sci. Lett.* **243**, 1 (2006). doi:10.1016/j.epsl.2005.12.017
73. H. Hikida, M. A. Wieczorek, Crustal thickness of the Moon: New constraints from gravity inversions using polyhedral shape models. *Icarus* **192**, 150 (2007). doi:10.1016/j.icarus.2007.06.015

**Acknowledgments:** The GRAIL mission is supported by the Discovery Program of the National Aeronautics and Space Administrations (NASA) and is performed under contract to the Massachusetts Institute of Technology and the Jet Propulsion Laboratory, California Institute of Technology. Additional support for this work was provided by the French Space Agency (CNES), the Centre National de la Recherche Scientifique, and the UnivEarthS LabEx project of Sorbonne Paris Cité. Data products will be made available from the authors upon request.

**Supplementary Materials**
www.sciencemag.org/cgi/content/full/science.1231530/DC1
Supplementary Text
Table S1
Figs. S1 to S13
References (*36–73*)

15 October 2012; accepted 27 November 2012
Published online 5 December 2012
10.1126/science.1231530

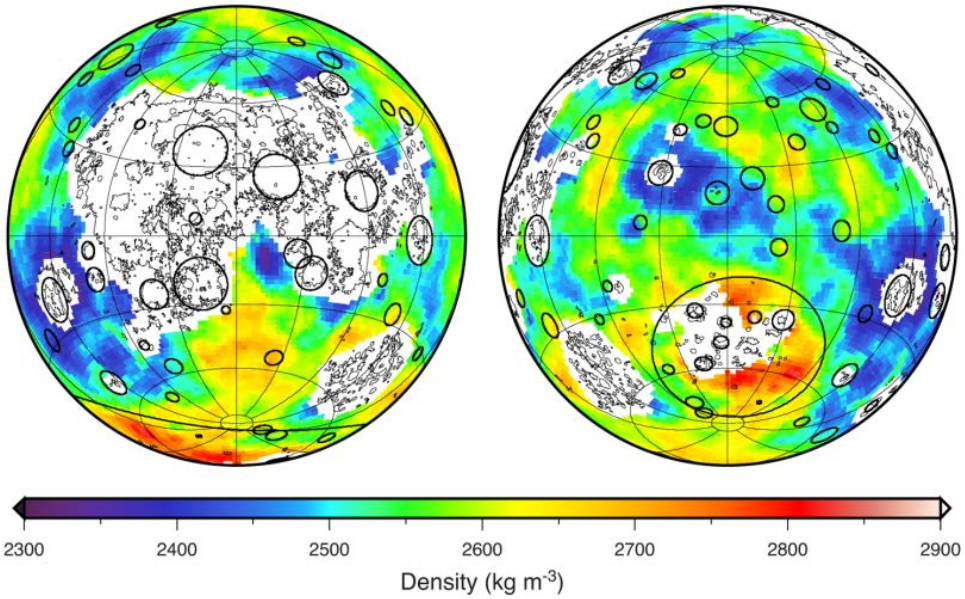


**Fig. 1.** Bulk density of the lunar crust from gravity and topography data. At each point on a grid of 60-km spacing, the bulk density was calculated within circles of 360 km diameter(spanning 12° of latitude). White denotes regions that were not analyzed, thin lines outline the maria, and solid circles correspond to prominent impact basins, whose diameters are taken as the region of crustal thinning in Fig. 3. The largest farside basin is the South Pole-Aitken basin. Data are presented in two Lambert azimuthal equal-area projections centered over the near- (left) and far- side (right) hemispheres, with each image covering 75% of the lunar surface, and with grid lines spaced every 30°. Prominent impact basins are annotated in Fig. 3.

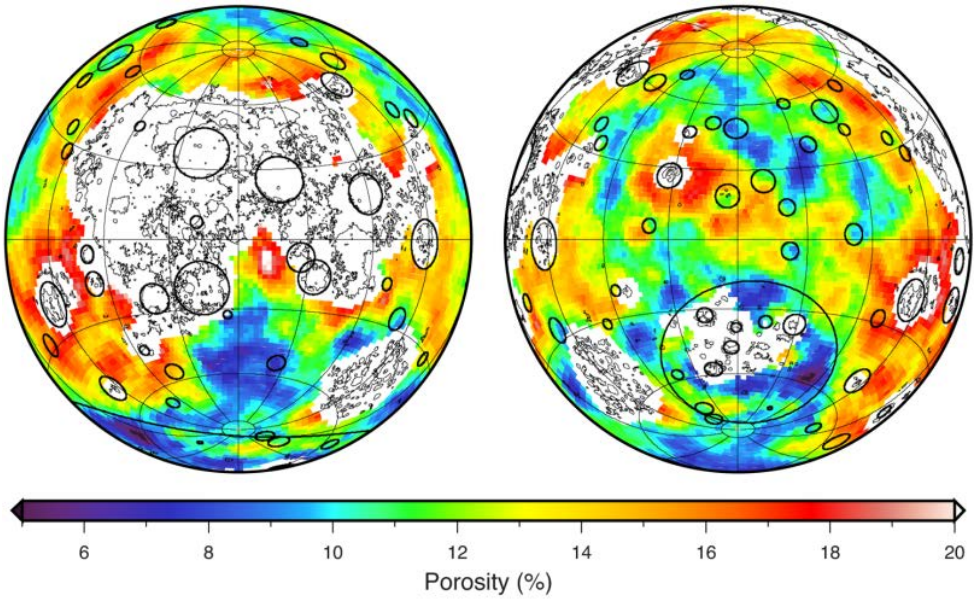


**Fig. 2.** Porosity of the lunar crust, using bulk density from GRAIL and grain density from sample and remote-sensing analyses. Image format is the same as in Fig. 1.

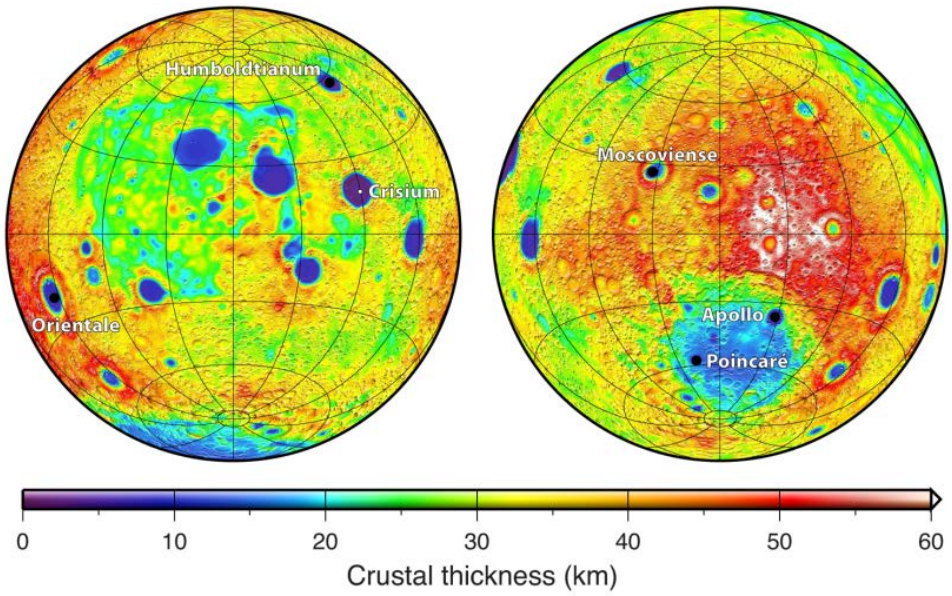


**Fig. 3.** Crustal thickness of the Moon from GRAIL gravity and LRO topography. With a crustal porosity of 12% and a mantle density of 3220 kg $m^{-3}$, the minimum crustal thickness is less than 1 km in the interior of the farside basin Moscoviense, and the thickness at the Apollo 12 and 14 landing sites is 30 km. Image format is the same as in Fig. 1, and each image is overlain by a shaded relief map derived from surface topography.